JOURNAL OF GEOPHYSICAL RESEARCH, VOL. 113, B05301, doi:10.1029/2007JB005034, 2008

Spectral analysis of seismic noise induced by rivers: A new tool to monitor spatiotemporal changes in stream hydrodynamics

A. Burtin,[1,2] L. Bollinger,[2] J. Vergne,[1] R. Cattin,[1] and J. L. Nábělek[3]

Received 8 March 2007; revised 19 September 2007; accepted 28 January 2008; published 2 May 2008.

[1] Analysis of continuous seismic data recorded by a dense passive seismological network (Hi-CLIMB) installed across the Himalayas reveals strong spatial and temporal variations in the ambient seismic energy produced at high frequencies (>1 Hz). From June to September 2003, the high-frequency seismic noise is observed to increase up to 20 dB (relative to $(m/s)^2$/Hz) for all the stations located along a steep 30-km-long narrow and deeply incised channel of the Trisuli River, a major trans-Himalayan river. The early summer increase in high-frequency energy is modulated by a 24-h periodicity where the minimum of seismic noise level is reached around noon and the maximum is reached late in the evening. A detailed study of seismic noise amplitude reveals a clear correlation with both regional meteorological and hydrological data along the Trisuli River. Seasonal increase in ambient noise coincides with the strong monsoon rainfall and a period of rapid melting of snow and ice in the high elevations. The observed 24-h cyclicity is consistent with the daily fluctuation of the precipitation and river discharge in the region. River-induced seismic noise is partly generated by stream turbulence, but this mechanism fails to explain the observed clockwise hysteresis of seismic noise amplitude versus water level. This pattern is better explained if a significant part of the observed seismic noise is caused by ground vibrations generated by bed load transport. This points out the potential of using background seismic noise to quantify in continuous river bed load and monitor its spatial variations, which remain difficult with classical approaches.

Citation: Burtin, A., L. Bollinger, J. Vergne, R. Cattin, and J. L. Nábělek (2008), Spectral analysis of seismic noise induced by rivers: A new tool to monitor spatiotemporal changes in stream hydrodynamics, *J. Geophys. Res.*, *113*, B05301, doi:10.1029/2007JB005034.

1. Introduction

[2] Assessing the level and the periodic variations of background seismic noise at seismological stations is of first importance to determine threshold limits for the detection and discrimination of seismic signals. As a result, there has been considerable interest in determining the nature of the seismic noise environment [e.g., *Brune and Oliver*, 1959] and the factors controlling it through large permanent seismological arrays [e.g., *Peterson*, 1993; *Stutzmann et al.*, 2000; *McNamara and Buland*, 2004; *Stehly et al.*, 2006] and temporary seismic networks [e.g., *Wilson et al.*, 2002; *de la Torre and Sheehan*, 2005]. It appears that the ambient seismic noise affects the entire frequency band studied in seismology from 10^{-3} to 10^{2} Hz. Here, we focus this study on mechanisms involved in seismic noise generation, which exhibit strong temporal variations at various periods.

[3] At low-frequency ($<10^{-1}$ Hz) sources are primarily natural, induced by local weather conditions, like diurnal temperature or atmospheric pressure variations [*Zürn and Widmer*, 1995; *Beauduin et al.*, 1996]. Some of the very low-frequency noise 10^{-3}–10^{-1} Hz has been attributed to infragravity waves, presenting seasonal fluctuations, mainly given to be generated by the ocean and controlled by the spatiotemporal variations of the storms over the oceans [*Rhie and Romanowicz*, 2004; *Schulte-Pelkum et al.*, 2004; *Stehly et al.*, 2006]. The oceanic source dominates through the "microseism" band, usually between 5×10^{-2}–10^{-1} Hz for the primary band [*Oliver and Ewing*, 1957] and 10^{-1}–2×10^{-1} Hz for the secondary band, producing a peak of noise amplitude at 0.2 Hz, visible anywhere on the Earth [e.g., *Longuet-Higgins*, 1950; *Gutenberg*, 1958; *Peterson*, 1993; *Stutzmann et al.*, 2000]. Early works of *Banerji* [1924, 1930] have also revealed the influence of regional weather condition, such as the southwest monsoon, on the amplitude of seismic noise produced in the microseism band.

[4] At high frequency (>1 Hz), seismic noise is mainly dominated by cultural sources [e.g., *Marzorati and Bindi*,

[1]UMR 8538 Laboratoire de Géologie, ENS, CNRS, Paris, France.
[2]Laboratoire de Détection et de Géophysique, CEA, Bruyères-le-Châtel, France.
[3]College of Oceanic and Atmospheric Sciences, Oregon State University, Corvallis, Oregon, USA.

0148-0227/08/2007JB005034$09.00

2006]. Traffic and industries are responsible for an important noise level and induce very strong diurnal variations [*McNamara and Buland*, 2004]. Among natural sources, winds can be considered as broadband sources, producing large amplitudes of noise at high frequencies (>1 Hz) [*Bahavar and North*, 2002] and important long-period noise on horizontal components [e.g., *Withers et al.*, 1996; *Young et al.*, 1996; *de la Torre and Sheehan*, 2005] encompassing fluctuations in response to the variation of the wind intensity [*Wilcock et al.*, 1999].

[5] In this paper, we analyze the data acquired by a large-aperture, densely spaced temporary seismic array set across the Himalayas and southern Tibet. Stations were sampling many kinds of seismic noise from cultural to natural sources. We focus our analysis on a segment following the trans-Himalayan Trisuli River, which is affected by monsoon rainfall and melting of snow and ice over one year. In the context of such strong meteorological and hydrological fluctuations, this data set is well suited for the study of the influence of rivers on the amount of seismic noise and its spatiotemporal variation, a critical issue in the Himalayas where Nepal Seismic Network shows strong spatiotemporal variations of its detection capacities [*Bollinger et al.*, 2007]. Rivers have long been recognized as sources of seismic noise but, to our knowledge, the mechanism responsible for coupling the river energy to seismic noise has never been explored. Following a brief description of the studied temporary network, we examine ambient seismic noise characteristics over one complete year, encompassing periods of large hydrological changes. We compare the ambient noise features to hydrological data and evaluate the potential of using seismic records for hydrological studies focused on bed load monitoring.

2. Data and Processing

2.1. Hi-CLIMB Seismic Data Acquisition

[6] This study is part of the Himalayan Tibetan Continental Lithosphere during Mountain Building experiment (Hi-CLIMB), a project designed to image the lithospheric structures across the Himalayan collision zone. During this 3-year experiment, 115 broadband seismometers were deployed over 280 sites from southern Nepal to the Banggong suture in central Tibet [*Nábělek et al.*, 2005; *Hetényi*, 2007]. The southern section of the network (named hereafter phase 1) consisted of 75 stations, with an interstation distance of about 3 km, installed from the Terai plain to southern Tibet along the south-north Birganj-Hetauda-Naubise road in order to keep a linear profile (Figure 1). Farther north, it reached the Betrawati-Dhunche-Syabru road along the Trisuli River. Stations H0010 to H0480, located in Nepal, were deployed from October 2002 to April 2004, whereas stations H0490 to H0770, located in south Tibet, where deployed from May 2003 to June 2004.

[7] Three types of seismometers (velocity meters) were used: broadband seismometers Streckeisen STS-2 and Guralp CMG-3T with a natural period of 120 s, and intermediate-band seismometers Guralp CMG-3ESP with a natural period of 33 s. All these instruments have a flat response up to 50 Hz. To compare results from different instruments, seismograms were corrected for instrument response. The REFTEK (72A08) 24-bit recording system had a sampling frequency of 50 Hz with an antialias, low-pass filter at 20 Hz. In addition to a thick soil cover, they have been thermally isolated with a 4 cm thick polystyrene insulation and glass wool.

[8] The environmental conditions are variable along the profile, with the proximity of towns and frequented roads especially for the southern stations (Terai basin), whereas in the Himalayan range large villages are rare, roads are infrequently traveled. The geological setting of the seismological stations also varies along the array. South of the Main Frontal Thrust (MFT) (stations H0010–H0120), the instruments are located in the Terai basin constituted of recent alluvial layers deposited over a molassic formation named the Siwaliks group formation [e.g., *Upreti*, 1999]. Farther north, from the north slopes of the Siwaliks hills to the high Himalayan range, the outcrops consist of granite, gneiss and high-grade rocks of the Kathmandu klippe (stations H0170–H0320), overlying lower grade lesser Himalayas metasediments [*Upreti*, 1999; *Bollinger et al.*, 2004] (stations H0330–H0430). Through the high Himalayan range, instruments (stations H0440–H0530) have been installed along the bottom of a narrow valley incised in crystalline rock units consisting mainly of gneisses and quartzites [*Upreti*, 1999]. Finally, in southern Tibet, stations (stations H0540–H0710) are located over the Tethysian sedimentary series.

2.2. Noise Power Spectral Density Estimation

[9] An example of two 1-d-long records from station H0460 (Figure 2), located in the vicinity of the Trisuli River, reveals large temporal variations of the seismic noise. During summer, high-frequency noise is one order larger than during winter. Moreover, a daily variation of the noise during summer is also noticed, with larger noise amplitude at night than during the day.

[10] To quantify the energy emitted at given frequencies from the seismic recordings, we computed the power spectral density (PSD) of the time series. The PSDs are calculated using Welch's averaging method [*Welch*, 1967]. The purpose of this power spectral estimator is to reduce the variance of spectra, dividing the time series in segments potentially overlapping. Segments are windowed using a Hamming window to avoid side effects when the signal is cut out. A modified periodogram [*Welch*, 1967] is calculated for each segment at given frequencies and the PSD is deduced from averaging the periodograms. The use of a multitaper method (MTM), usually offering greater frequency resolution and variance properties, do not significantly improve the analysis results. Small differences, never exceeding 5% for the frequency range studied here, argued therefore for the lower time consuming Welch's overlapped segmented average techniques (Figure S1 of the auxiliary material).[1]

[11] Two procedures were used for enhancing the different timescales in the observed fluctuation of ambient noise level, from hours to seasons. The first approach consists of extracting a full-day recording, subdivided into 1-h-long segments with 50% overlap. A PSD is then calculated over each window and averaged to obtain a daily spectrum. This procedure is used to study the spatial evolution of noise

[1] Auxiliary materials are available in the HTML. doi:10.1029/2007JB005034.

Figure 1. Location of the study area in central Nepal and southern Tibet. Main cities, Hi-CLIMB seismological stations as well as Department of Hydrology and Meteorology of Nepal (DHM) meteorological stations used in this study are represented by circles, inverse triangles, and diamonds, respectively. MCT, MBT, and MFT refer to Main Central Thrust, Main Boundary Thrust, and Main Frontal Thrust, respectively.

energy by averaging each daily PSD through the entire year. The window length and the sampling rate were a good compromise between the computation time and the spectrum resolution required to obtain a small variance at all frequencies. The second procedure consists in extracting records of 10-min length subdivided into eight 75-s-long segments with no overlap. This method serves to characterize the rapid temporal variations of the energy produced at a given frequency. Once again, the choice of the sampling rate and the window length with no overlap is efficient to get an accurate resolution of PSDs with a reasonable calculation time. These procedures were applied to data from each station component and results are given in decibels [dB] relative to the velocity ($10 \times \log_{10}[(\mathrm{m/s})^2/\mathrm{Hz}]$).

3. Spatial to Temporal Variations of Ambient Seismic Noise

3.1. Spatial Evolution

[12] The long-term PSDs for 2003 at a set of stations selected to sample the typical ambient seismic noise and local geology across Nepal and southern Tibet are shown on Figure 3. These stations include station H0050 underlain by low-velocity sediment layers [*Hetényi et al.*, 2006] on a foreland basin; station H0230 located on the Kathmandu klippe crystalline unit of high Himalayan affinity; as well as stations H0460 and H0660 in the High Himalaya and southern Tibet, respectively. The noise levels are compared to the world noise bounds determined by the low- and high-noise models of *Peterson* [1993].

[13] As expected, station H0050, located in a densely populated area and installed on soft sediments, is the noisiest station over the entire frequency band (Figure 3). Horizontal components display energy amplitudes systematically larger by 20 dB than at stations located north of the MFT, and the microseismic peak at 0.2 Hz is more pronounced. Low-frequency noise (<0.2 Hz) remains almost constant for stations located north of the MFT, as depicted by the noise spectra at stations H0230, H0460 and H0660 (Figure 3). All these stations are installed on bedrock. These observations point the role played by local geology on the amplitude of seismic noise, like the presence of low-velocity sediments south of the MFT, which probably produce strong waveguide layers to seismic waves.

[14] In the high-frequency band (>1 Hz), the energy decreases up to 50 dB from south (station H0050) to north (station H0660) meaning that the noise level is diminished by a factor of 300. This noise decrease is consistent with a northward decrease in population density from Nepal to Tibet (Landscan, 2005, http://www.ornl.gov/sci/landscan/index.html), hence a similar decrease in anthropogenic

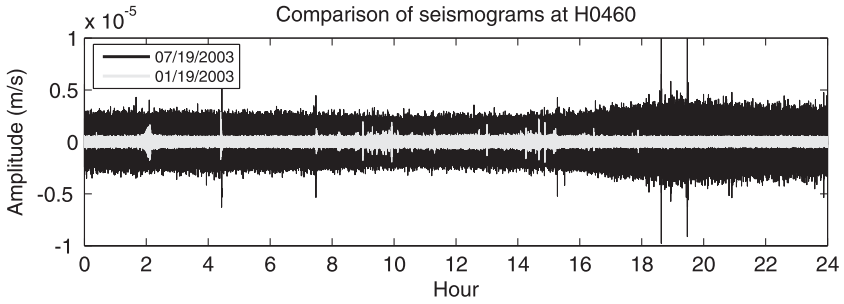

Figure 2. Comparison of two 1-d-long vertical seismograms recorded at station H0460. A full day of January (19 January 2003) and July (19 July 2003) are represented in white and black, respectively. The data are presented in local time. In January the level of background noise is constant during the day, except some perturbations probably due to cultural noise. In July the background noise level is one order larger than in January and depicts fluctuations within a day where a maximum amplitude is observed in the evening.

noise sources across the Himalayas [*de la Torre and Sheehan*, 2005]. However, almost all stations from H0410 to H0570 exhibit a noise level energy, in the frequency band ~2–12 Hz, equivalent to what is observed with southern stations. This feature is illustrated with stations H0460 on Figure 3, this station having a similar noise level energy at high frequencies as H0230. Since these stations are located far from any major cities and high traffic roads, the origin of this seismic noise, in this frequency band, cannot be linked to anthropogenic sources and is rather related to natural sources.

3.2. Seasonal Variations

[15] The analysis of seasonal background noise modulation may help differentiating processes of seismic noise generations that can be associated with natural sources, at least climatic ones. Figure 4 presents the seasonal fluctuation computed with the first procedure of PSD calculation and the difference realized on the average PSDs for the month of July and February for a given station. In the microseism band (0.1–1 Hz), stations H0050, H0230, and H0460 record larger energy amplitudes in July by about 5 to 10 dB (Figure 4). The appearance of oceanic depressions localized over the Gulf of Bengal during the summer monsoon period [e.g., *Lang and Barros*, 2002] could explain the enhancement of oceanic swell and thus the larger amplitudes of the 0.2 Hz peak [*Banerji*, 1930]. Although still visible, this effect is attenuated for the northern stations on the Tibet plateau, like H0660 (Figure 4).

[16] The main seasonal noise variation is seen in the high-frequency band (>1 Hz) for station H0460 with an average increase of 15 dB during summer, whereas stations H0050 and H0230 do not show any significant seasonal changes in this frequency band (Figure 4). The noise amplitudes on the seismograms from station H0460 are then 6 times larger at high frequency during the monsoon period than during the dry season (Figure 2). A similar observation is made at most stations located along the Trisuli River.

3.3. Daily Fluctuation

[17] The above analysis is too coarse to study the mechanism of possible background noise induced by rivers, for this we look at daily variations. In Figure 5a, we present the spatial and temporal evolution of the seismic noise level at all the Hi-CLIMB stations located close to the Trisuli River. For each station, we calculate the daily high-frequency energy on the vertical component over a chosen frequency band (Figure 5b). The center and the width of the selected band have been chosen based on the frequencies that are visibly excited during the summer months. For stations where no obvious seasonal variations are observed, the default 2–10 Hz band is chosen.

[18] The daily noise levels during 2003 at stations close to the Trisuli River, reveals a strong increase of the high-frequency energy (>1 Hz), from stations H0410 to H0560 (Figure 1) from June to September (Figure 5a). For these stations, the level of noise shows a first increase at the end of May lasting until mid-June. Then, the energy reveals a second increase and reaches an almost constant level until the end of September with intermittent peaks that are well correlated between stations. The time period of energy enhancement coincides with the summer monsoon period in Nepal, during which depressions centered over the Gulf of Bengal [e.g., *Barros and Lang*, 2003] place the Himalayan arc under a regime of moist southeast flow and produce important episodes of heavy rainfall. From early June to end of September, the cumulative precipitation can reach 5 m in western Nepal, at the front of the High Himalayan range [*Department of Hydrology and Meteorology* (*DHM*), 2002]. Stations showing pronounced seasonal seismic noise fluctuations are located nearby river segments with steep local gradients (Figure 5c), whereas at the northern and southern ends of the Trisuli River covered by the Hi-CLIMB network, the summer increase of high-frequency energy is attenuated or not visible (Figure 5).

[19] The annual three-component PSDs through year 2003 at high frequencies are displayed in Figure 6 for stations located along the Trisuli River. The summer enhancement of the high-frequency energy is seen at all components. However, the amplitude of seismic noise and the bandwidth of the excited frequencies are larger on the horizontal than on the vertical component recordings (Figure 6). Two steps of increasing noise level are seen in June while a wider band of frequencies is progressively excited. This widening of the noise band is mainly observed at lower frequencies (stations H0420, H0460, and H0470, Figure 6).

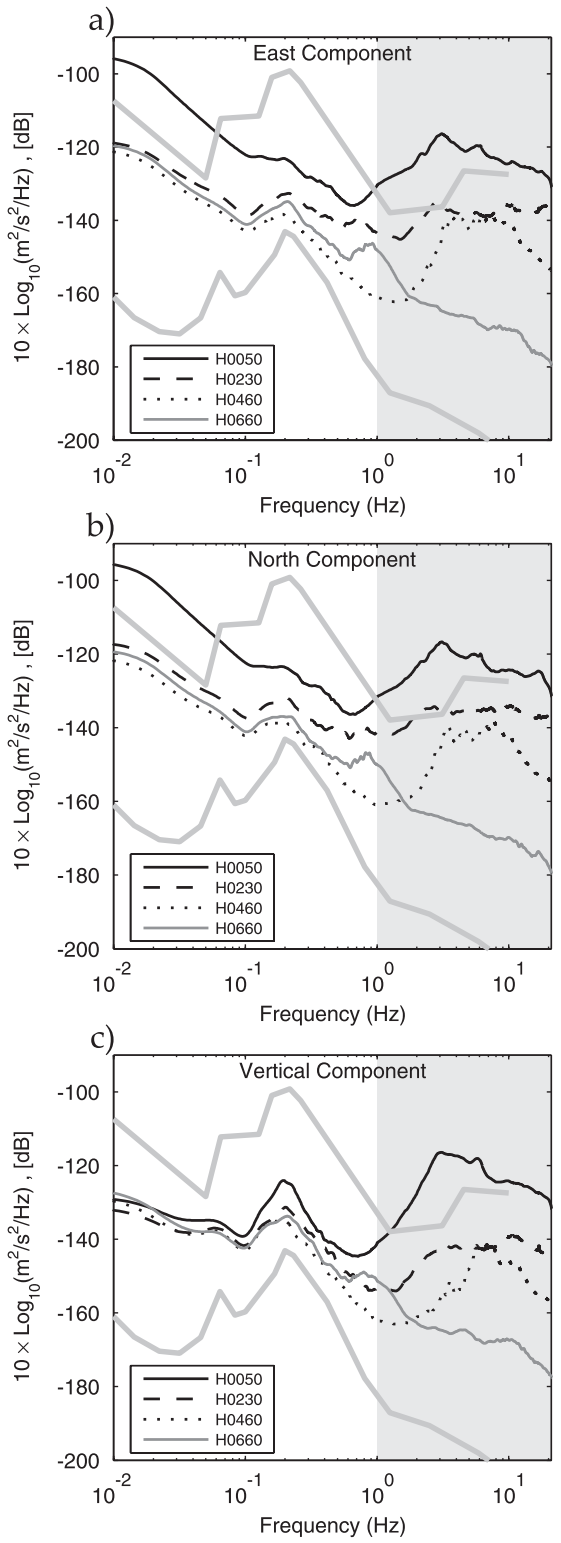

Figure 3. Mean annual (2003) PSDs estimated for four stations H0050, H0230, H0460, and H0660 from south to north, respectively (Figure 1) for (a) east, (b) north, and (c) vertical components. The large gray lines are the new high noise model (NHNM) and the new low noise model (NLNM) of *Peterson* [1993]. The amplitudes are given in decibel [dB] relative to velocity ($10 \times \log_{10}[(m/s)^2/Hz]$). Gray shaded area indicates the frequency band (1–20 Hz), considered in this study.

[20] The hourly fluctuation of the summer high-frequency energy is shown in Figure 7. The appearance of the summer seismic noise coincides with the appearance of a 24-h period cycle and is superposed to a constant increase of the daily average noise level. This 24-h cycle has a minimum amplitude reached at 01 pm and a maximum amplitude late in the evening (Figures 7 and 8). This suggests that the source responsible for this seismic noise is anticorrelated with the possible sources of anthropogenic noise, which has a minimum at night. This 24-h periodic signal is observed from stations H0440 to H0510 covering about 30 km along the Trisuli River (Figure 8). South of station H0420 and north of H0510, the diurnal modulation of the summer seismic noise at high frequencies is not present. These "low-noise" regions coincide with areas where the gradient of the river stream is small (Figure 5).

4. Discussion

[21] The proximity of the Trisuli River to stations showing seasonal variations of energy at high frequencies suggests an interaction between the source of noise and the river discharge. To test this hypothesis we compare local meteorological and hydrological data with the noise level curves obtained from the seismic stations installed along the river. Although some hydrological studies and monitoring have been conducted in the past along the upper Trisuli [e.g., *DHM*, 1998; *Sharma and Adhikari*, 2004] and the Langtang Khola, one of its major tributaries [*Fukushima et al.*, 1987; *Takahashi et al.*, 1987], the river discharge and sediment load remain largely unmonitored. For this reason, we first introduce the meteorological context of the study region for year 2003, precipitation water being one of the main contributors to the Langtang-Trisuli river hydrology [e.g., *Braun et al.*, 1993, 1998]. We next introduce the available water level time series and discuss the complementary hydrological data set.

4.1. Comparison With Meteorological Data

[22] We compare the precipitation rates (mm/d) calculated with a 10-d moving average for 8 meteorological stations monitored by the Department of Hydrology and Meteorology of Nepal (DHM) located along the Trisuli River (white diamonds on Figure 1) with the average integrated energy on the velocimeter's three components and over a significantly excited frequency band (3–15 Hz) at stations H0420, H0460 and H0480 for year 2003 (Figure 9). We focus on these specific stations located through the area encompassing large summer increase of the high-frequency noise (Figure 5) because they almost operated continuously during the experiment. From January to May the precipitation in the region are rare and weak meanwhile the noise level is low. However, the noise level time series does not correlate with the rare local rainfall (Figure 9). In June at the onset of the monsoon season, the precipitation rate increases and remains at the highest levels of the year until the end of September. In June, seismic noise at the observed stations increases rapidly, reaching an amplitude threshold for the following three months. At the end of September, the precipitation rates depict a sudden decrease whereas the recession of ambient noise is gentler (Figure 9). The overall

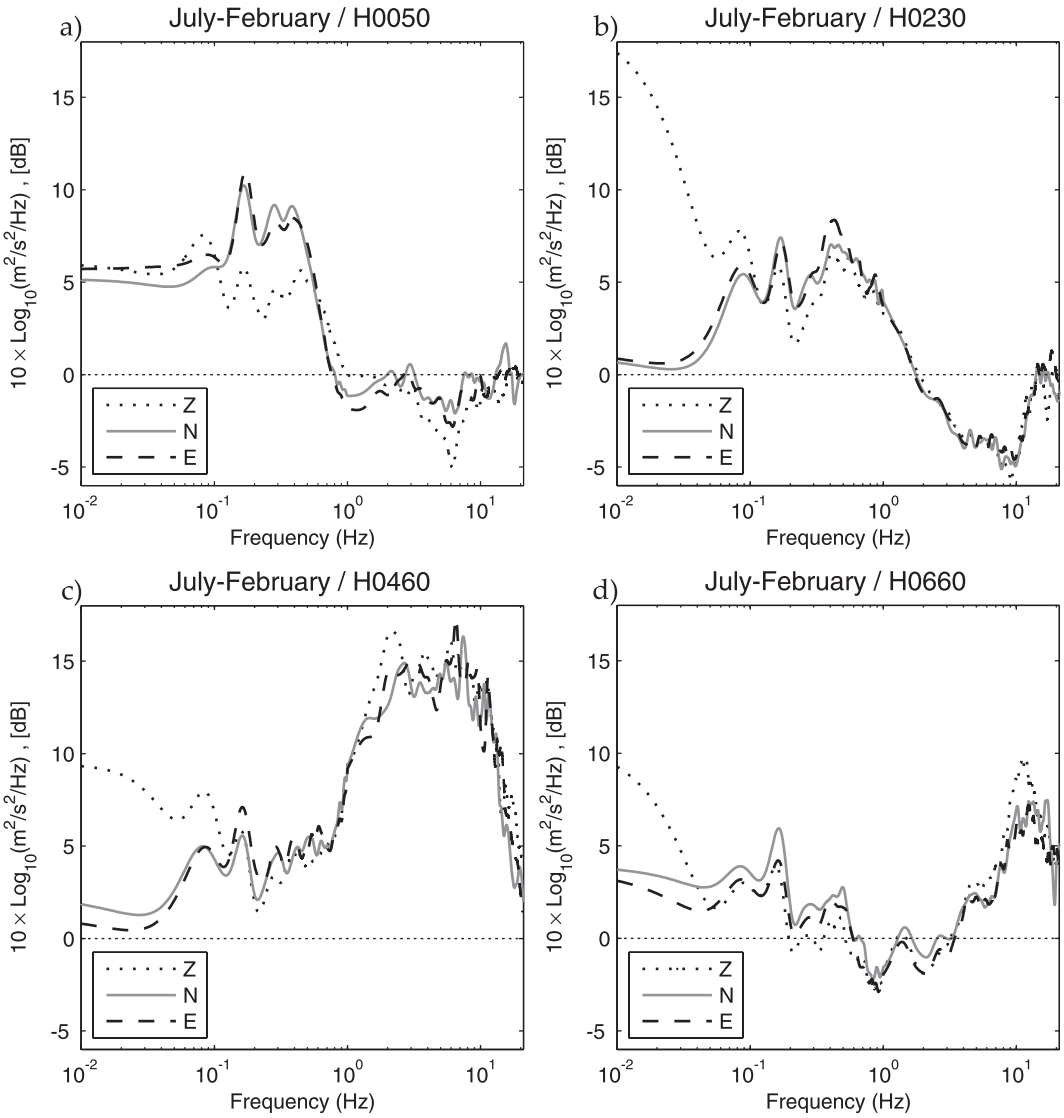

Figure 4. Seasonal fluctuation of seismic noise: obtained by subtracting the average July PSD to the average February PSD for 2003 at stations (a) H0050, (b) H0230, (c) H0460, and (d) H0660. Black dotted, gray continuous, and black dashed lines represent the vertical, north, and east components, respectively. The amplitudes are given in decibel [dB] relative to velocity ($10 \times \log_{10}[(\mathrm{m/s})^2/\mathrm{Hz}]$).

correlation coefficient between noise amplitude at H0460 with precipitation is 0.61.

[23] Monitoring hourly precipitation at an automatic weather station in Syangboche (Khumbu-eastern Nepal) at 3850 m, *Ueno et al.* [2001] show a remarkably periodic diurnal cycle during the summer monsoon. The total amount of precipitation from 04 pm to 06 am corresponds to 88% of the daily total amount. This result is supported by complementary observations made at higher altitudes (at the Pyramid Meteorological station at 5050 m) in the same region [*Bollasina et al.*, 2002] and farther west along the Annapurna range by a 16-station hydrometeorological network [*Barros et al.*, 2000; *Barros and Lang*, 2003]. [*Barros and Lang*, 2003] indicate that the main peak of precipitation in the Annapurna region comes around midnight, the minimum of rain being generally observed between 06 am and noon. This diurnal precipitation periodicity during the summer monsoon might thus be systematic along the front of the high range in Nepal and appears to be closely tied to our observations of the daily seismic noise variations along the Trisuli River (Figures 7 and 8).

[24] Although the daily fluctuations of monsoon rainfall are in phase with the diurnal pattern of seismic noise observed at stations along the Trisuli River, we notice some discrepancies between noise level and precipitation rates over longer periods. For instance in April and May, the seismic noise gently increases whereas average precipitation rates do not differ from previous months (Figure 9). Similarly, the noise from October to December remains at a higher level than during the period preceding the summer monsoon, whereas episodes of rain are essentially nonexistent. Finally, peaks of noise level during the monsoon period are not well in phase with peaks of precipitation (Figure 9).

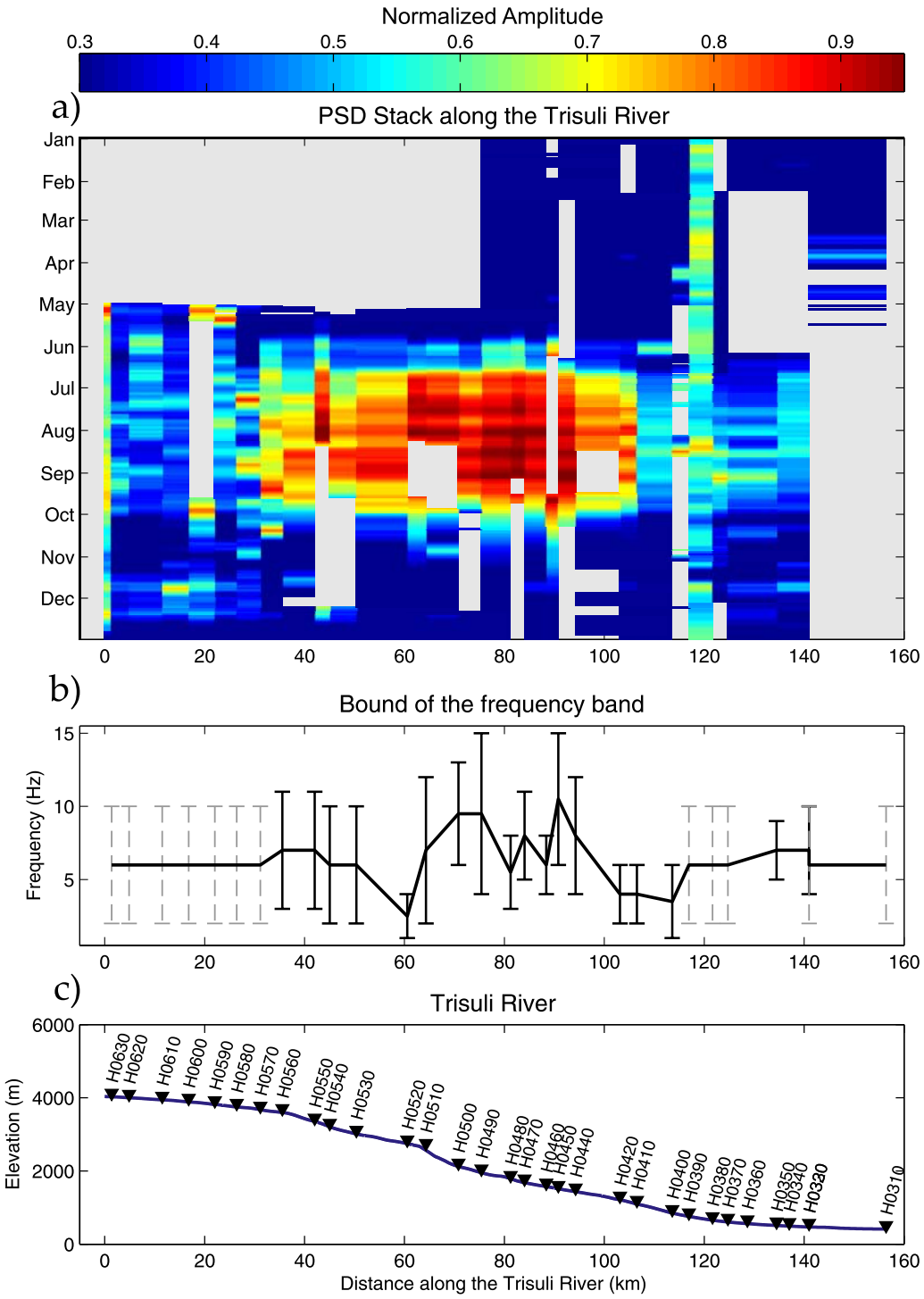

Figure 5. (a) Mean vertical PSDs at Hi-CLIMB stations along the Trisuli River and stacked over the frequencies excited in summer, given in Figure 5b. PSDs are rescaled between 0 and 1, minimum and maximum PSDs amplitudes, respectively, and smoothed with a centered sliding window of 2 weeks. Red and blue represent high and low normalized energy, respectively. (b) Center of the chosen frequency band along the Trisuli River for the PSD stacks (black line). The black error bars stand for the lower and upper bound of the stacked frequencies. The gray dashed error bars mark the default values of the upper and lower frequency bound (2–10 Hz) when the summer increase of the high-frequency energy is not clearly identified. (c) Location of the Hi-CLIMB stations (downward black triangles) projected on the elevation profile of the Trisuli river (blue line).

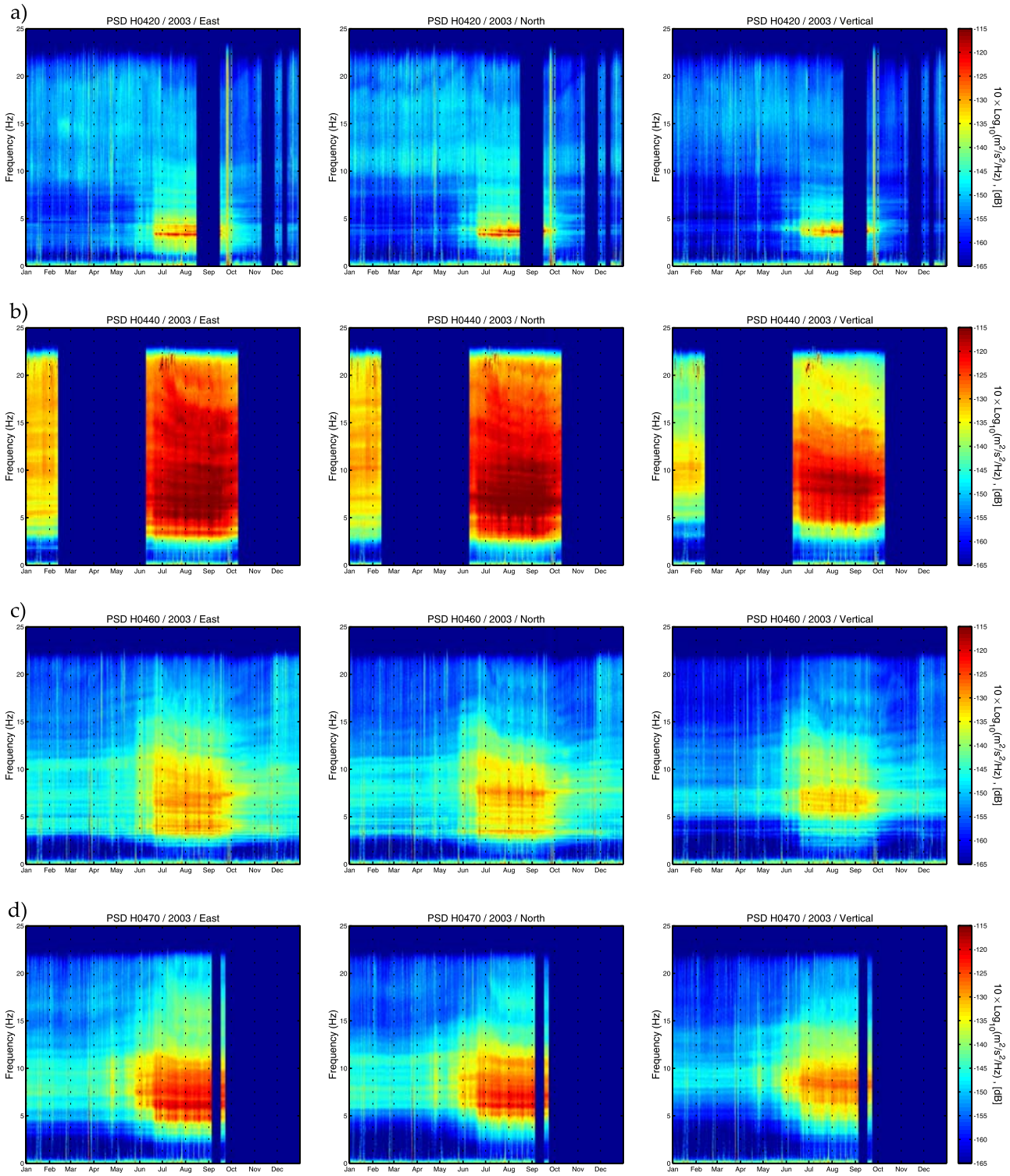

Figure 6. Spectrograms for the east, north, and vertical components for the year 2003 at stations (a) H0420, (b) H0440, (c) H0460, and (d) H0470. Each vertical stripe corresponds to a PSD estimated for a 1-h-long data segment (see the text for details of the procedure). Red and blue stand for high and low energy, respectively.

4.2. Comparison With Hydrological Data

[25] Monsoon rainfall is not the only supply of water for Himalayan rivers, melting snow and ice are also major additional contributors. *Fukushima et al.* [1987] presented a study of the Langtang valley in which three glacier watersheds were instrumented from July 1985 to June 1986. Some hydrological studies have been conducted in rather similar Himalayan hydrological contexts, p.e. in the vicinity of the Garhwal glaciers and the river they feed [e.g., *Singh et al.*, 2003, 2005], describing large diurnal and seasonal

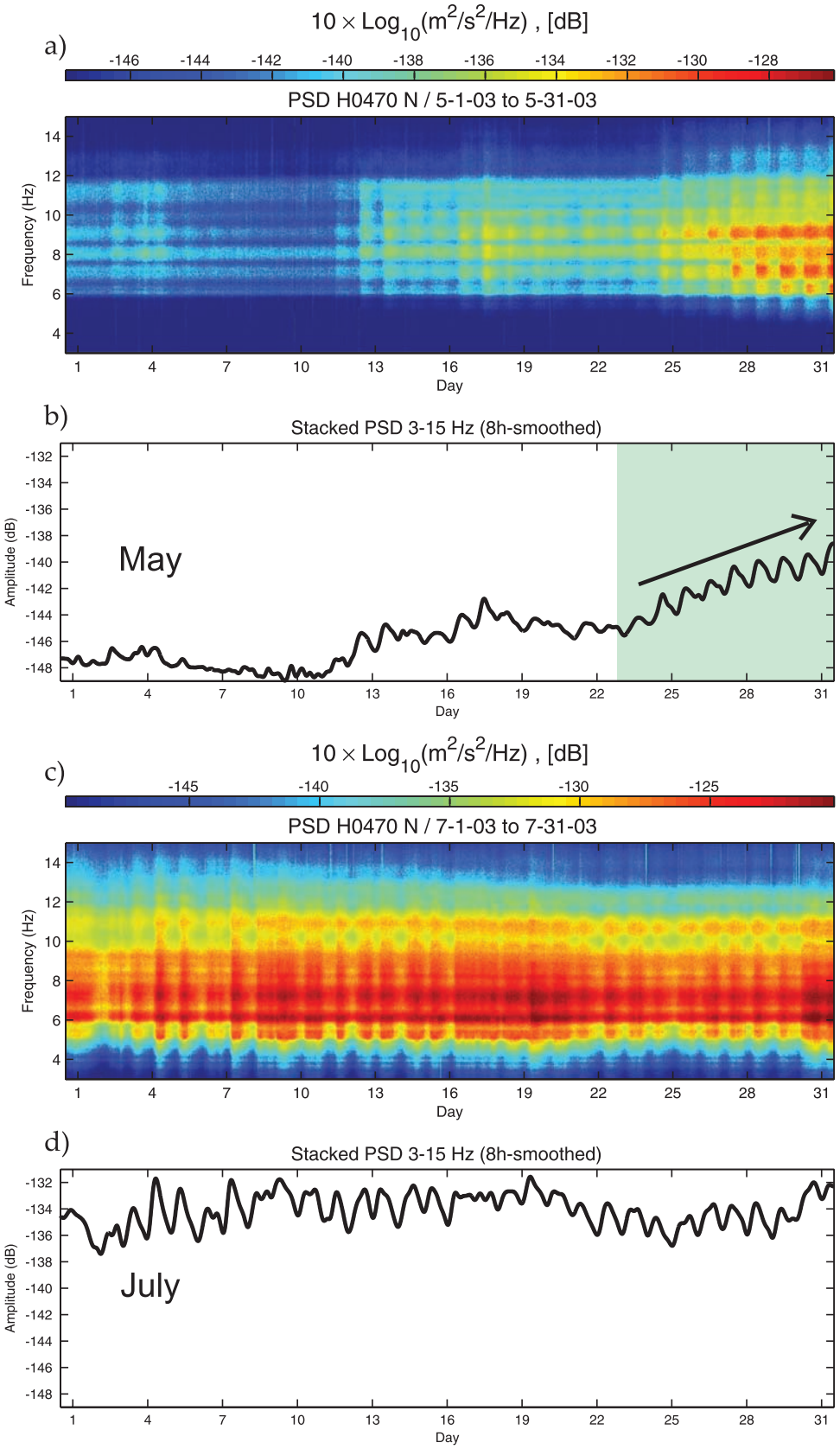

Figure 7. (a) Spectrograms for May 2003 at station H0470. Each vertical stripe corresponds to a PSD for a 10 min data segment (see the text for details of the procedure). Red and blue stand for high and low energy, respectively. (b) Corresponding mean PSDs stacked over a frequency band of 3–15 Hz and smoothed with an 8-h sliding window. Green shaded area in Figure 7b depicts the onset of the 24-h periodicity and the constant increase of the seismic noise. (c–d) Same as Figures 7a and 7b but in July 2003.

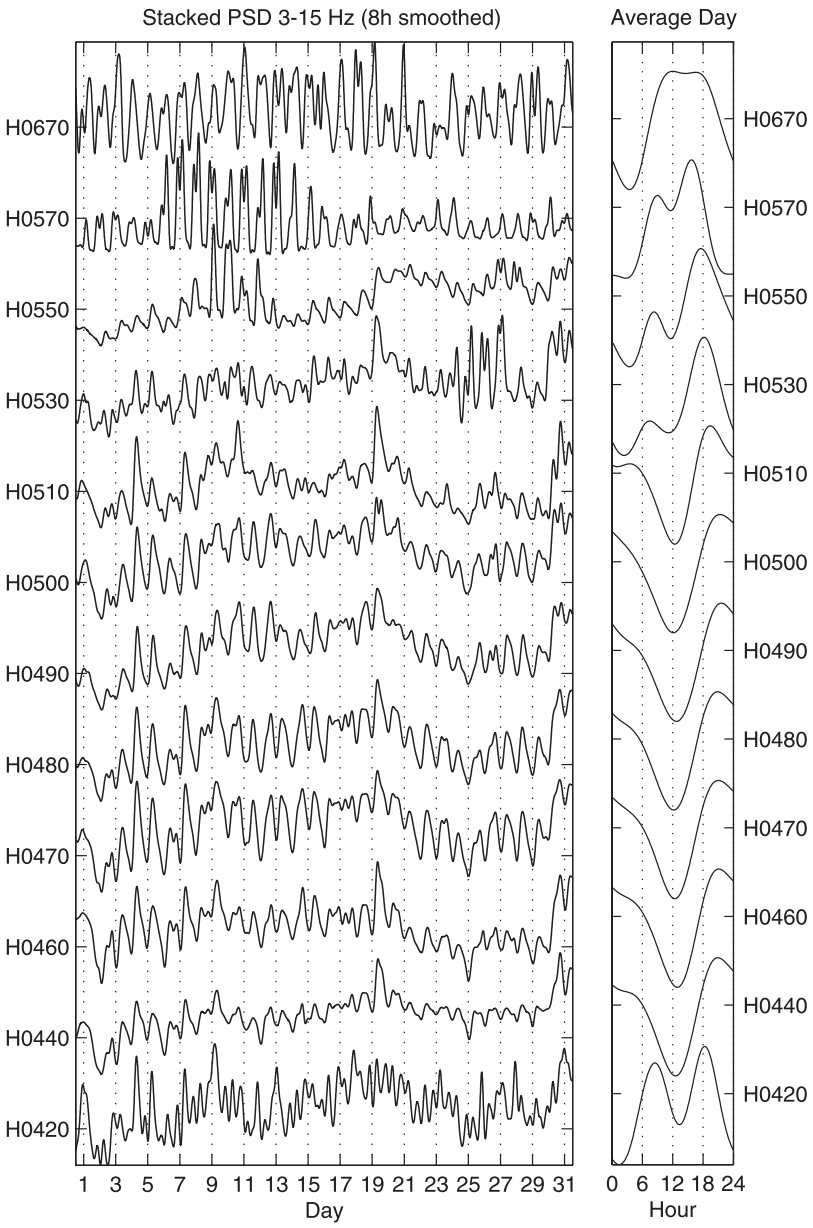

Figure 8. (a) PSDs stacked over a frequency band of 3–15 Hz for July 2003 and for a set of Hi-CLIMB stations from north to south, top to bottom, respectively. (b) Corresponding mean daily noise level variations calculated by summing 24-h-long segments of the curves shown in Figure 8a. The 24-h periodicity, with maximum noise around 2200 LT, is observed along a segment of 30 km along the Trisuli River. North and south of it, the cyclicity is typical of cultural sources with a maximum reached during the day.

variations in discharge and sediment fluxes, including runoff delaying and hysteresis trends between discharge and the suspended sediment concentrations. Continuous measurements of the discharge of the largest tributary to the Trisuli River the Langtang Khola (Figure 1) during this period show a gentle increase of discharge from April to May followed by a rapid augmentation in June due to the fast melting of snow and ice in glaciers in response to increased air temperature [*Takahashi et al.*, 1987]. In July and August, discharge rates reach the largest values, followed in September to October by a period of rapid discharge recession, whereas from November to March the discharge decreases only slightly. [*Fukushima et al.*, 1987] also observe a daily fluctuation of discharge during July and August. According to them, the hourly discharge rate is the largest from 09 pm to midnight in the Langtang Khola watershed. These seasonal and daily variation of discharge measurements seem to be well correlated with our observations of noise levels at seismic stations close to the Trisuli River. Unfortunately, there is a lack of continuous and reliable water discharge measurements along the Trisuli River, except a measurement of the daily water level variations in the town of Betrawati, close to station H0370. Furthermore, to our knowledge, this transport is not monitored on regular basis along the Trisuli River. Total dissolved solids (TDS) episodic measurements at Betrawati

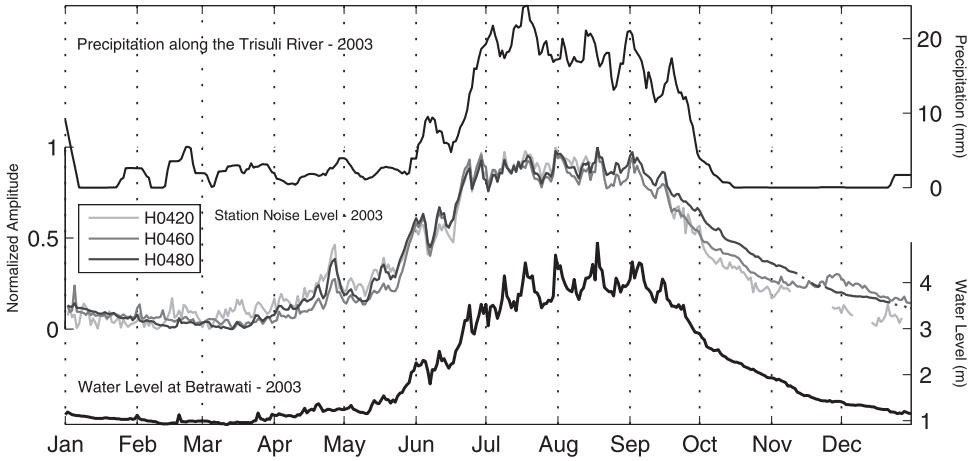

Figure 9. Top curve is the 10-d centered moving average of the daily precipitation rate in mm for year 2003 at 8 meteorological stations from the Department of Hydrology and Meteorology of Nepal (DHM) located along the valley of the Trisuli River (Figure 1). Middle curves are the high-frequency noise level (averaged over the three components and the frequency band 3–15 Hz for year 2003) at stations H0420, H0460, and H0480. Bottom curve is the Trisuli water level in meters measured at the town of Betrawati near station H0370 during year 2003.

barrage in 1993–1994 depict seasonal variations, with a peak of amplitude in July August around 5 times higher than the fall-spring values [*Galy and France-Lanord*, 1999]. Considerably greater variations are suspected for the suspended sediments [e.g., *Evans et al.*, 2004] while almost all the bed load transport is given to be accommodated during the summer monsoon. On Figure 9, we compare the integrated water level at this hydrological station with the integrated seismic noise level estimated at stations H0420, H0460 and H0480. From January to April, both recordings keep a constant level with a few sudden increases of water level that does not match to noise level, except perhaps one in early February. As from the middle of May, water and seismic noise levels undergo increases during which fluctuations are well correlated, for example, the rapid and strong recession of noise and water level observed in the first part of June. During the monsoon period, the time series of both data sets is well correlated. As mentioned earlier, the daily precipitation rate variations could not fully explain the seismic noise variations (Figure 9). Moreover, at the end of September, when the precipitation rapidly decreases, the decrease in noise level follows the similar slower diminution of water level. Overall, the correlation coefficient between H0460 seismic noise and water level is 0.86, whereas it is only 0.61 with precipitation.

4.3. Sources of "River" Seismic Noise

[26] The correlation between seismic noise and water level clearly suggests that the main source of seismic noise during the monsoon period is linked to the variations in the stream power of the Trisuli River along its fast flowing portion in the High Himalaya zone. The accommodation of the water supply from precipitation or snow/ice melt may vary dramatically along the Trisuli River due to variations of the watershed and the evolution of the river geometry from north to south. South of station H0370, the river has a weak gradient and a wide channel, up to 100 m during the monsoon, and the supply of water is mainly accommodated by an increase of the width. On contrary, through the High Himalayan range, the river has a strong gradient and the channel is narrow, around 10 m. Flanked by steep slopes, the large amount of water supplied by the monsoon is mainly balanced by an increase of the water level, which enhances the basal shear stress of the Trisuli River. The fluvial shear stress exerted by the flowing water is defined as

$$\tau = \rho g R S, \tag{1}$$

where ρ is the fluid density, g is the gravity, S is the water surface slope, and R the hydraulic radius. R can be expressed as the function of the channel width W and the water level H in the approximation of a rectangular section:

$$R = \frac{WH}{(W + 2H)}. \tag{2}$$

Thus, assuming a constant section, an increase in H produces a much higher increase in basal shear stress than an increase in W. One effect of the increase in the basal shear stress is the initiation of the bed load motion.

[27] The correlation of the integrated seismic noise with the water level of the river reveals that the hydrodynamics is a possible source of seismic noise. Because of a larger river discharge during the monsoon, the turbulence induced by the stream is probably at the origin of the observed seismic noise. In Figure 10, the plot of the seismic noise level at H0420, H0460, and H0480 as a function of the water level for the whole year 2003 reveals a well-developed hysteresis pattern. This result shows that for equivalent water level the amplitude of noise recorded at the beginning of the monsoon (June to July) is larger than the one recorded at the end of the rain season (September to October). If turbulent flow is the only source of seismic noise, one would expect a linear trend between amplitude of seismic noise and water level. No large variation of high-frequency seismic noise should be observed between the beginning and the ending

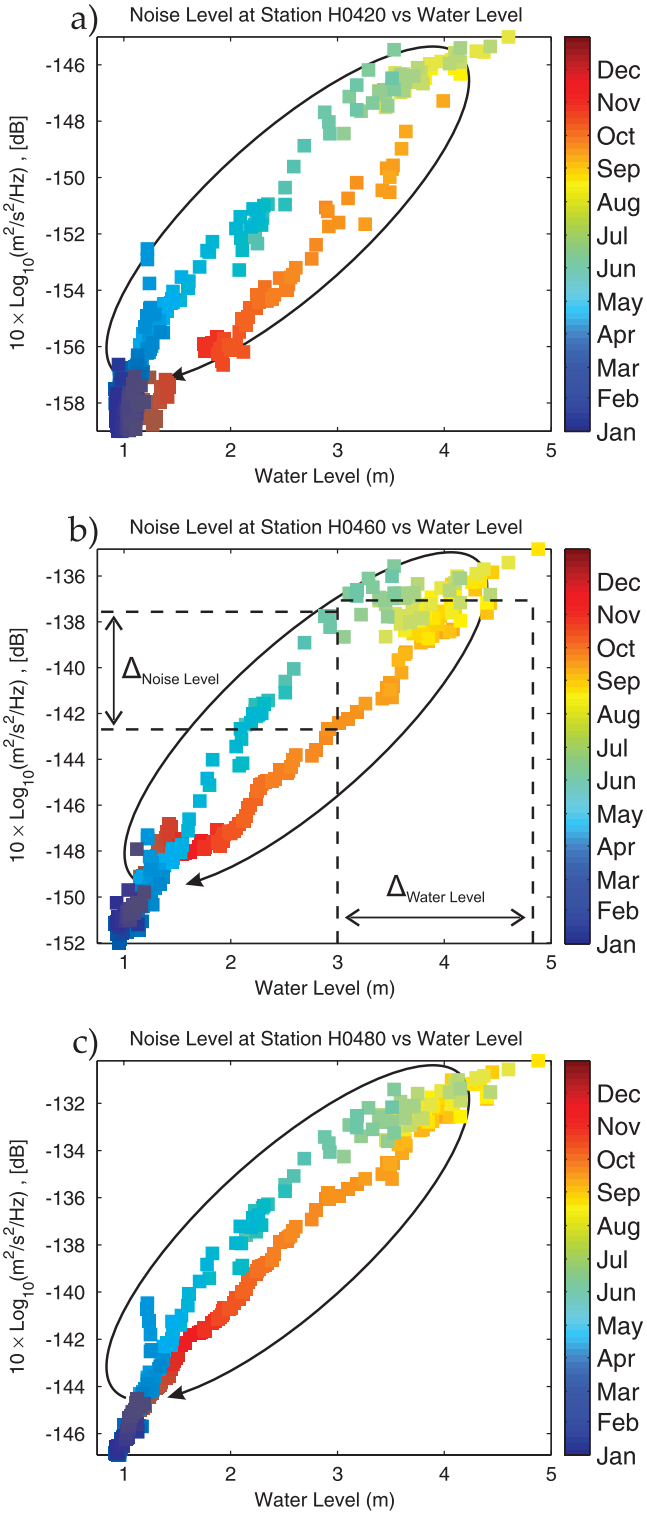

Figure 10. Mean daily noise level amplitudes at station (a) H0420, (b) H0460, and (c) H0480 compared to the daily water level of the Trisuli River measured at Betrawati during year 2003. Each square represents 1 d, and its color indicates month of the year. The observed hysteresis progression is indicated by the black arrow curve.

of the summer monsoon. However, the hysteresis pattern demonstrates that the stream turbulence cannot be the unique source of high-frequency seismic noise.

[28] Through the high range where the Trisuli valley is well incised and water supply is mainly accommodated vertically, the river gradient is steep (Figure 5), the bed load is coarse and consists of large boulders. On the other hand, farther south, where river gradient is gentler and the channel is wider, the bed load is finer, consisting of smaller pebbles. This spatial variability of the bed load type along the Trisuli River, caused by the variations of its hydrodynamics, seems related with the north-south variations of the high-frequency seismic signal that we observe at stations along the flow. We suspect that part of the available bed load at the beginning of the rainfall season have been used or removed at the end of the monsoon, which leads to a decrease in the river-generated seismic noise, since only the largest boulders remain available to produce noise. Moreover, from July to August, despite a constant increase in water level (from 3.25 to 5 m), the amplitude of the noise remains almost constant (<2 dB). This threshold behavior of seismic noise energy reminds the classical concept of critical shear stress used to describe the river transport capacity [e.g., *du Boys*, 1879; *Shields*, 1936]. If the stress of the flowing water is less than the critical shear stress, particles within the river will remain motionless. Only when the stress exerted by the flowing water exceeds the critical shear stress, movement will be observed. If motion of all the available river bed load is already involved, an increase in water level should have no influence on seismic noise.

[29] North of station H0560, noise levels do not show any variation correlated to the monsoon period. It can be explained by a weak river discharge due to rain shadow effects of the range or by the higher altitudes of this region, which reduce the amount of water coming from snow and ice melt. Furthermore, despite of the major effect of monsoon rainfall in the water supply south of Betrawati, we do not have significant seasonal changes in the amplitude of noise. Stations in the southern part of the river are located in the vicinity of river segments for which the bed load characteristics are not efficient to produce seismic noise either due to a missing large fraction of the bed load or variations of the basal shear stress.

[30] All these observations point the influence of the different mechanisms of bed load transport on the recorded seismic noise. The motion of blocks within the river should produce seismic waves since this solid fraction is coupled to the ground.

5. Conclusions

[31] Our study reveals that some hydrodynamics features of the Trisuli River can be assessed from the temporal/frequency analysis of continuous seismic records at Hi-CLIMB stations installed along its bank. On the basis of our observations, motion of the bed load on the river bedrock, including pebble saltation or bed load creep, is a plausible mechanism for the generation of the observed high-frequency seismic noise, which suggests that seismometers can be used to monitor bed load transport. Furthermore, recent work by [*Huang et al.*, 2007] shows, using time-frequency analysis of ground vibration in an experimental context, that

some seismic noise in the 10–150 Hz band is generated by rock motions. Both observations let us suspect that the bed load transport in the rivers is an important contributor to the seismic noise in the vicinity of large rivers. This type of load transport is one of the most efficient mechanisms of erosion and is a major cause of damage during high floods. The evaluation of the river bed load remains difficult to quantify due to a potential strong hydrodynamics. The Hi-CLIMB network, not being designed for such a purpose, lacked configuration which would facilitate more accurate evaluation of the bed load transport along this trans-Himalayan river. Furthermore, independent estimates of the bed load were also lacking, but our study points out the potentials of this new approach. Seismic-based measurements of bed load can potentially overcome some of the weakness of commonly used methods in an extreme flowing water environment. First, the presented method is noninvasive because seismometers are deployed outside the river channel. In our study, some stations (H0410, H0420, etc.) were installed at more than 2 km from the river and still exhibit a clear river-generated noise. Hence, ambient seismic noise analysis can be used as a tool to continuously monitor the river bed load transport. Second, we observe a wide range of frequencies that are excited during the monsoon period, which indicates that the frequency content of the river seismic noise can potentially help to characterize the nature of the bed load and its type of motion (saltation, shearing, etc.). Third, since seismic records at one station are sensitive to a broad portion of the river near it, measurement of noise energy, corrected from the geometrical and intrinsic local attenuation, can provide an integrated value of the bed load transport along the river. Assuming that a sufficiently dense network of stations with a specific geometry including both perpendicular and transversal profiles is installed at the scale of a local watershed, restricted areas of high bed load transport can thus be localized with tomography-like inversion techniques. Finally, and perhaps most importantly, seismic data can be transmitted in almost real-time and the long-term experience of the seismological community in the rapid determination of earthquake location and magnitude determination can potentially be used, in complementary with existing methods, in warning systems for destructive floods.

[32] **Acknowledgments.** The authors would like to thank the entire Hi-CLIMB team for the fieldwork and data acquisition. We are grateful to the Department of Hydrology and Meteorology of Nepal for providing the hydrological data. We thank J. Lavé, J.-P. Avouac, and K. Whipple for discussions and P. Molnar and E. Saygin for their valuable comments and suggestions on the manuscript. Project Hi-CLIMB is supported by the U.S. NSF Continental Dynamics Program, EAR 9909609.

References

Bahavar, M., and R. North (2002), Estimation of background noise for international monitoring system seismic stations, *Pure Appl. Geophys.*, *159*, 911–944.

Banerji, S. K. (1924), Microseisms associated with the incidence of the south-west monsoon, *Nature*, *114*, 576.

Banerji, S. K. (1930), Microseisms associated with disturbed weather in the Indian seas, *Philos. Trans. R. Soc. London, Ser. A*, *229*, 287–328.

Barros, A. P., and T. J. Lang (2003), Monitoring the monsoon in the Himalayas: Observations in central Nepal, June 2001, *Mon. Weather Rev.*, *131*, 1408–1427.

Barros, A. P., M. Joshi, J. Putkonen, and D. W. Burbank (2000), A study of the 1999 monsoon rainfall in a mountainous region in central Nepal using TRMM products and rain gauge observations, *Geophys. Res. Lett.*, *27*(22), 3683–3686.

Beauduin, R., P. Lognonné, J. P. Montagner, S. Cacho, J. F. Karczewski, and M. Morand (1996), The effects of the atmospheric pressure changes on seismic signal or how to improve the quality of a station, *Bull. Seismol. Soc. Am.*, *86*(6), 1760–1769.

Bollasina, M., L. Bertolani, and G. Tartari (2002), Meteorological observations at high altitude in the Khumbu Valley, Nepal Himalayas, 1994–1999, *Bull. Glaciol. Res.*, *19*, 1–11.

Bollinger, L., J.-P. Avouac, O. Beyssac, E. J. Catlos, T. M. Harrison, M. Grove, B. Goffé, and S. Sapkota (2004), Thermal structure and exhumation history of the Lesser Himalaya in central Nepal, *Tectonics*, *23*, TC5015, doi:10.1029/2003TC001564.

Bollinger, L., F. Perrier, J.-P. Avouac, S. Sapkota, U. Gautam, and D. R. Tiwari (2007), Seasonal modulation of seismicity in the Himalaya of Nepal, *Geophys. Res. Lett.*, *34*, L08304, doi:10.1029/2006GL029192.

Braun, L., W. Grabs, and Rana (1993), Application of a conceptual precipitation-runoff model in the Langtang Khola Basin, Nepal Himalaya, *IAHS Publ.*, *218*, 221–237.

Braun, L. N., Ch. Hottelet, M. Weber, and W. Grabs (1998), Measurement and simulation of runoff from Nepalese head watersheds, *IAHS Publ.*, *248*, 9–18.

Brune, J. N., and J. Oliver (1959), The seismic noise of the Earth's surface, *Bull. Seismol. Soc. Am.*, *49*(4), 349–353.

de la Torre, T. L., and A. F. Sheehan (2005), Broadband seismic noise analysis of the Himalayan Nepal Tibet seismic experiment, *Bull. Seismol. Soc. Am.*, *95*(3), 1202–1208, doi:10.1785/0120040098.

Department of Hydrology and Meteorology (DHM) (1998), Hydrological records of Nepal, streamflow summary, report, 264 pp., Kathmandu, Nepal.

Department of Hydrology and Meteorology (DHM) (2002), Daily precipitation records of Nepal 1999–2000, report, 274 pp., Kathmandu, Nepal.

du Boys, M. P. (1879), Étude du régime du Rhône et de l'action exercée par les eaux sur un lit à fond de graviers indéfiniment affouillable, *Ann. Ponts Chaussees*, *5*(18), 141–195.

Evans, M. J., L. A. Derry, and C. France-Lanord (2004), Geothermal fluxes of alkalinity in the Narayani river system of central Nepal, *Geochem. Geophys. Geosyst.*, *5*, Q08011, doi:10.1029/2004GC000719.

Fukushima, Y., K. Kawashima, M. Suzuki, T. Ohata, H. Motoyama, H. Kubota, T. Yamada, and O. R. Bajracharya (1987), Runoff characteristics in three glacier-covered watersheds of Langtang Valley, Nepal Himalayas, *Bull. Glacier Res.*, *5*, 11–18.

Galy, A., and C. France-Lanord (1999), Weathering processes in the Ganges-Brahmaputra basin and the riverine alkalinity budget, *Chem. Geol.*, *159*, 31–60, doi:10.1016/S0009-2541(99)00033-9.

Gutenberg, B. (1958), Microseisms, *Adv. Geophys.*, *5*, 53–92.

Hetényi, G. (2007), Evolution of deformation of the Himalayan prism: from imaging to modelling, Ph.D. thesis, 400 pp., École Normale Supérieure–Univ. Paris-Sud XI, Paris.

Hetényi, G., R. Cattin, J. Vergne, and J. L. Nábělek (2006), The effective elastic thickness of the india plate from receiver function imaging, gravity anomalies and thermomechanical modelling, *Geophys. J. Int.*, *167*, 1106–1118, doi:10.1111/j.1365-246X.2006.03198.x.

Huang, C.-J., H.-Y. Yin, C.-Y. Chen, C.-H. Yeh, and C.-L. Wang (2007), Ground vibrations produced by rock motions and debris flows, *J. Geophys. Res.*, *112*, F02014, doi:10.1029/2005JF000437.

Lang, T. J., and A. P. Barros (2002), An investigation of the onsets of the 1999 and 2000 monsoons in central Nepal, *Mon. Weather Rev.*, *130*, 1299–1316.

Longuet-Higgins, M. S. (1950), A theory of the origin of microseisms, *Philos. Trans. R. Soc. London*, *243*, 1–35.

Marzorati, S., and D. Bindi (2006), Ambient noise levels in north central Italy, *Geochem. Geophys. Geosyst.*, *7*, Q09010, doi:10.1029/2006GC001256.

McNamara, D. E., and R. P. Buland (2004), Ambient noise levels in the continental United States, *Bull. Seismol. Soc. Am.*, *94*(4), 1517–1527, doi:10.1785/012003001.

Nábělek, J. L., J. Vergne, G. Hetényi, and the Hi-CLIMB Team (2005), Project Hi-CLIMB: A synoptic view of the Himalayan collision zone and southern Tibet, *Eos Trans. AGU*, *86*(52), Fall Meet. Suppl., Abstract T52A-02.

Oliver, J., and M. Ewing (1957), Microseisms in the 11- to 18-second period range, *Bull. Seismol. Soc. Am.*, *47*(2), 111–127.

Peterson, J. (1993), Observation and modeling of seismic background noise, *U.S. Geol. Surv. Open File Rep.*, *93-322*, 1–95.

Rhie, J., and B. Romanowicz (2004), Excitation of Earth's continuous free oscillations by atmosphere-ocean-seafloor coupling, *Nature*, *431*, 552–556, doi:10.1038/nature02942.

Schulte-Pelkum, V., P. S. Earle, and F. L. Vernon (2004), Strong directivity of ocean-generated seismic noise, *Geochem. Geophys. Geosyst.*, *5*, Q03004, doi:10.1029/2003GC000520.

Sharma, K., and N. Adhikari (2004), Hydrological estimations in Nepal, report, 104 pp., Dep. of Hydrol. and Meteorol., Kathmandu, Nepal.

Shields, A. (1936), Anwendung der Aehnlichkeitsmechanik und der Turbulenzforschung auf die Geschiebebewegung, *Mitt. Preuss. Versuchsanst. Wasserbau Schiffbau*, *26*, 26. (English translation by W. P. Ott and J. C. van Uchelen, 36 pp., U.S. Dep. of Agric. Soil Conser. Serv. Coop. Lab., Calif., Inst. of Technol., Pasadena, 1936.)

Singh, P., K. S. Ramasatri, N. Kumar, and N. K. Bhatnagar (2003), Suspended sediment transport from the Dokriani Glacier in the Garhwal Himalayas, *Nord. Hydrol.*, *34*(3), 221–244.

Singh, P., U. K. Haritashya, K. S. Ramasastri, and N. Kumar (2005), Diurnal variations in discharge and suspended sediment concentration, including runoff-delaying characteristics, of the Gangotri Glacier in the Garhwal Himalayas, *Hydrol. Processes*, *19*(7), 1445–1457, doi:10.1002/hyp.5583.

Stehly, L., M. Campillo, and N. M. Shapiro (2006), A study of the seismic noise from its long-range correlation properties, *J. Geophys. Res.*, *111*, B10306, doi:10.1029/2005JB004237.

Stutzmann, E., G. Roult, and L. Astiz (2000), GEOSCOPE station noise levels, *Bull. Seismol. Soc. Am.*, *90*(3), 690–701.

Takahashi, S., H. Motoyama, K. Kawashima, Y. Morinaga, K. Seko, H. Iida, H. Kubota, and N. R. Tradahr (1987), Summary of meteorological data at Kyangchen in Langtang Valley, Nepal Himalayas, 1985–1986, *Bull. Glacier Res.*, *5*, 121.

Ueno, K., et al. (2001), Meteorological observations during 1994–2000 at the Automatic Weather Station (GEN-AWS) in Khumbu region, Nepal Himalayas, *Bull. Glaciol. Res.*, *18*, 23–30.

Upreti, B. N. (1999), An overview of the stratigraphy and tectonics of the Nepal Himalaya, *J. Asian Earth Sci.*, *17*(5), 577–606, doi:10.1016/S1367-9120(99)00047-4.

Welch, P. D. (1967), The use of fast Fourier transform for the estimation of power spectra: A method based on time averaging over short, modified periodograms, *IEEE Trans. Audio Electroacoust.*, *15*(2), 70–73.

Wilcock, W. S. D., S. C. Webb, and I. T. Bjarnason (1999), The Effect of local wind on seismic noise near 1 Hz at the MELT site and in Iceland, *Bull. Seismol. Soc. Am.*, *89*(6), 1543–1557.

Wilson, D., J. Leon, R. Aster, J. Ni, J. Schlue, S. Grand, S. Semken, S. Baldridge, and W. Gao (2002), Broadband seismic background noise at temporary seismic stations observed on a regional scale in the southwestern United States, *Bull. Seismol. Soc. Am.*, *92*(8), 3335–3341, doi:10.1785/0120010234.

Withers, M. M., R. C. Aster, C. J. Young, and E. P. Chael (1996), High frequency analysis of seismic background noise as a function of wind speed and shallow depth, *Bull. Seismol. Soc. Am.*, *86*(5), 1507–1515.

Young, C. J., E. P. Chael, M. M. Withers, and R. C. Aster (1996), A comparison of high frequency (>1 Hz) surface and subsurface noise environment at three sites in the United States, *Bull. Seismol. Soc. Am.*, *86*(5), 1516–1528.

Zürn, W., and R. Widmer (1995), On noise reduction in vertical seismic records below 2 mHz using local barometric pressure, *Geophys. Res. Lett.*, *22*(24), 3537–3540.

L. Bollinger, Laboratoire de Détection et de Géophysique, CEA, BP12, Bruyères-le-Châtel, F-91680, France.

A. Burtin, R. Cattin, and J. Vergne, Laboratoire de Géologie, École Normale Supérieure de Paris-CNRS, 24 rue Lhomond, F-75231 Paris Cedex 05, France. (burtin@geologie.ens.fr)

J. L. Nábělek, College of Oceanic and Atmospheric Sciences, Oregon State University, Corvallis, OR 97331, USA.